Atmospheric Pollution Research 11 (2020) 894–902

HOSTED BY

Contents lists available at ScienceDirect

Atmospheric Pollution Research

journal homepage: www.elsevier.com/locate/apr

Original Article

Characterization and behavior of Hydrogen Sulfide plumes released from active sulfide-tar springs, Hit-Iraq

Bayan Muhie Hussien[a], Muwafaq Ayesh Rabeea[b,*], Marwan Mohammed Farhan[b]

[a] Department of Environmental Sciences, College of Applied Sciences-Hit, University Of Anbar, Hit, 31007, Anbar, Iraq
[b] Department of Applied Chemistry, College of Applied Sciences-Hit, University Of Anbar, Hit, 31007, Anbar, Iraq

ARTICLE INFO

Keywords:
Air pollution
Dispersion
H_2S emission
Sulfide springs

ABSTRACT

The characteristics and behavior of the H_2S pollution plume in the emission zone of spring water and wastewater are determined by a total of 120 readings of H_2S in the air and 24 samples of dissolved gas analysis during the observation period. Monitoring data is adjusted to determine the behavior of air pollution plumes and their relationship to emission sources by using statistical techniques and spatial analysis. The value of H_2S emissions to the atmosphere was 6.62 kg/year by an emission factor of 0.0055 mg/s. The study revealed an important correlation between the continuous emission of H_2S and its sources from springs and wastewater that is explained by exponential relation Fit ($Y = a\ e^{bX}$), [H_2S concentration. In air (mg/1000 cc)] = 0.00015 exp {0.0107 (H_2S conc. In water mg/l)}. The spatial distribution maps of H_2S showed that 38% of Hit's space is exposed to H_2S concentration under the influence of the unpleasant odor, eye irritation, and corrosion in infrastructure parts (air conditioning apparatus). The characteristics of the H_2S pollution plume, which were reflected in the behavior of H_2S distribution of the exposed area, varied due to the variation of dispersion processes resulting from wind speed change. The concentration of H_2S was 11.6 times when the wind speed decreased by 15.7 times. The wind speed affected the results of the mechanical dispersion coefficient in a positive relationship. Vertical and horizontal mechanical dispersion values in unstable weather conditions increased by 192 times and 243 times than in extremely stable weather conditions.

1. Introduction

The study of air pollution was conducted in the Hit city west of the Euphrates River with a total area of (9) km^2 (Fig. 1). Hit city has a population of more than 100,000 people, suffers from continuous exposure to different levels of Hydrogen Sulfide (H_2S) concentration. The major sources of emissions are from sulfuric spring water Sayala spring (S) and Ilttayif spring (E) and along their flux, including their mixing zone with wastewater in Bassaer and Hummadi valley down to their confluence in the Euphrates River.

H_2S is a highly poisonous gas and was not classified as a greenhouse gas. It is identified by its distinctive odor “rotten eggs” and eye irritation, which occurs with increased exposure to gas at a concentration of 25–100 ppm, depending on individual sensitivity and duration of exposure. However, H_2S effect on the eye is less pronounced in places where exposure to the environment is at low-level and long-term. H_2S can be very dangerous and has been able to cause pneumonia (Schneider et al., 1998; D'Alessandro et al., 2012), sudden loss of consciousness (> 500 ppm) or death through exposure, if the levels are above 1000 ppm (Chi et al., 2019), and in a few minutes may cause respiratory paralysis because H_2S can be oxidized rapidly in the body. The permanent effects of acute exposure do not appear if the victim was immediately rescued and resuscitated.

Frequent exposure to low levels of H_2S may result in chronic respiratory symptoms, fatigue, headaches, and poor memory (Legator et al., 2001; Kari et al., 2019). A study in Iceland has shown that the H2S concentration more than 7.00 $\mu g/m^3$ caused increased visits to hospitals due to heart diseases (Finnbjornsdottir et al., 2016). Long exposure of H_2S at about 0.01–0.03 ppm is evident of impaired lung function or chronic obstructive pulmonary disease (Bates et al., 2015), and H_2S concentration of 2 ppm may cause bronchial obstruction in people with asthma (Jappinen et al., 1990). The normal low alarm level of warning in personal alarm sensors worn by workers in Sewage is at the Norwegian threshold of 5 ppm (Austigard et al., 2018). Either long-term or low-level emissions of H_2S concentrations can cause health deterioration. Studies by Cornelius et al. (2001) and Lantz et al. (2003)

Peer review under responsibility of Turkish National Committee for Air Pollution Research and Control.
* Corresponding author.
E-mail address: muw88@uoanbar.edu.iq (M.A. Rabeea).

https://doi.org/10.1016/j.apr.2020.02.001
Received 4 September 2019; Received in revised form 23 January 2020; Accepted 1 February 2020
Available online 06 February 2020

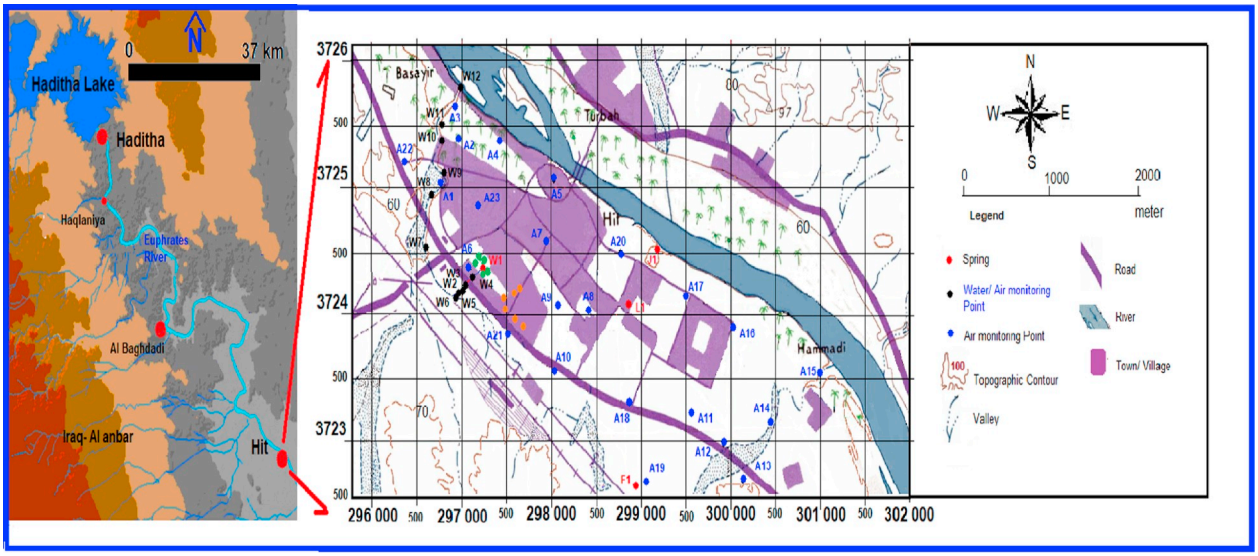

Fig. 1. Location map of the study area.

have not shown any evidence that the risk of asthma increases with exposure to H_2S. Proposals of risk reduction of high exposure areas with recent evidence suggested that H_2S has significant impacts on the body as it stimulates smooth muscle relaxation and reduces inflammation. No proven studies showed a relationship between H_2S and the increased risk of asthma. Because H_2S is formed below the land surface and its high solubility under pressure in the groundwater, it is released to the atmosphere throughout springs causing environmental problems. It may quickly attack the metal pipes and the valves of the equipment. A small concentration of H_2S can be economically harmful and require plant installation to remove H_2S and prevent corrosion (Selley and Sonnenberg, 2015).

The objective of this research is to identify the phenomenon of air pollution in Hit city resulting from the emission of H_2S originated from spring water and tar leakage. In addition, to evaluate the behavior of H_2S plumes dispersion on the basis of its effects in municipal, health, and engineering services (infrastructure, machinery, and equipment), where Hit city has important advantages as a region to study potential H_2S effects.

1.1. Hydrogeology of the H_2S emission zone

The region is subject to the effects of dry desert climate with the least impact of the Mediterranean climate and the Arabian Gulf. Depending on the results of the hydro-meteorological model (Hussien, 2010), the mean annual rainfall, evaporation, and temperature are ranged from 100 to 125 mm, 1900–2100 mm, and 24–25 °C, respectively. The study area is located within the Abu-Jir Fault zone in the transitional zone between the stable and unstable shelf. This subsurface right-lateral strike-slip fault was activated in the Late-Tertiary age extending north-south east (NSE) within the regional distribution zone of springs (Hijlan-Razzaza).

The geological Formations (Fns) of the Miocene-Quaternary period are exposed in the study area, including the Euphrates Formation (Fn) at a thickness of 47 m, consisting of dolomitic limestone and chalky marly limestone. It is overlain by Fatha Fn which consists of limestone, gypsum, claystone, and marl with a thickness of 5–23 m. The sediment of the Quaternary period consists of Pleistocene-Holocene sediment with a thickness of 0–5 m like slope, residual soils, valleys, plains, and Sabkha sediments.

Sulfide springs (SSp) are a source of H_2S air pollution within the study area, which has been characterized by a syntactic transition in terms of thickness and rock deformation between Arabian plate sediments (stable shelf) and Euphrates Graben sediments (unstable shelf) within the intersection of the Faults.

Limestone rocks with limited extensions of Fatha Fn are classified as perched aquifer with very low productivity. It is recharged by rainwater and deepest source (Hussien and Gharbi, 2010a). The water-bearing horizons of successive porous limestone and dolomitic limestone of the Euphrates Fn were classified as a semi-confined aquifer. However, Ana aquifer is composed of fractured, brecciated, fossiliferous porous dolomitic limestone. It is characterized by confining to semi-confined storage condition with high productivity.

Previous study (Hamza, 1975) has shown that the source of H_2S associated with hydrocarbons originated from the Cretaceous-Jurassic sediments (65–135 million years ago), such as Pilsner, Naher Omar, and Shu'aybah Fns, or from Ana and Aleeje Fns of the Oligocene age between 25 and 37 million years, after migration through Abu-Jir Fault zone. Which occurred at the end of the Alpine orogeny in Mio-Pliocene period (12 million years ago). Hydrocarbons (Tar and H_2S) are still leaking through SSp which are located on a level < 70 m above sea level within the last zone of the regional groundwater discharge. The discharge of the spring water was between 1 and 100 L/s and tar production ranged from 0.2 to 2 metric tons/day. Water salinity concentrations ranged from 4000 to 42,820 mg/L, while the concentration of the dissolved H_2S ranging from 12.5 to 428.5 mg/L (Al Dulaymie et al., 2013). Moreover, the hydro-geochemical results (Hussien and Gharbi, 2010b) indicated that the springs are classified as calcium; sulfate-chloride and sodium; sulfate-chloride water type. In addition, the source of water is from the mixing of oil field water with meteoric water and shallow groundwater. Also, it is observed that the most saline water is within the discharge zone, which belongs to the old deep groundwater.

H_2S emission in the study area is from S (Image-A; Northing 3,724,272; Easting 297,315) and from E (Image-B; Northing 3,722,359; Easting 298,922). Its water discharge is 35 L/s and 6 L/s and with dissolved H_2S concentration of 305 and 260 mg/L respectively (Al Dulaymie et al., 2013). These SSp are characterized by continuous water flow with alternating bubbles of H_2S gas, which can be identified by its odor and ignition. The spongy tar floats on the surface of the flowing water through the drainage channel towards Bassir and Hummadi valleys for S and E springs which later confluences into the Euphrates River.

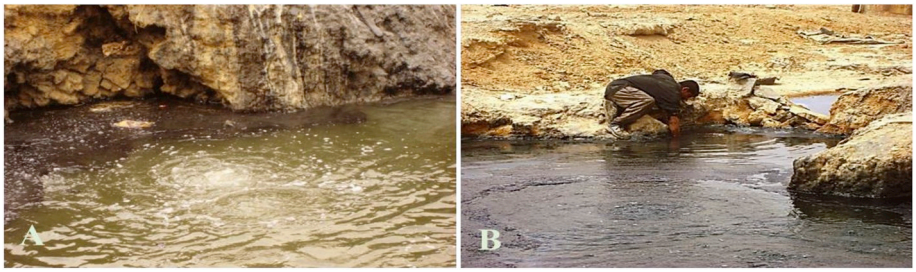

Image **A-** Sayala Spring and **B-** Ilttayif Spring.

1.2. Origin of Hydrogen Sulfide

In nature, H_2S is produced by bacterial processes during the degradation of both plant and animal protein, therefore it is commonly contaminated in sewage plants. Also, H_2S is produced from the direct reduction of sulfate water. Hydro geochemically, springs water was classified as sulfide water since that H_2S concentration in it exceeded 10 mg/L (Awadh and Abdul-Ghani, 2013).

H_2S is originated from the oil (bitumen) field water flowing like spring water in Hit and the surrounding area. The H_2S gas is formed as a result of the following oxidation and reduction reactions:

$$SO_4^{-2} + CH_4 \rightarrow HS^- + HCO_3^- + H_2O$$

$$HS^- + H_2O \rightarrow H_2S + OH^-$$

$$SO_4^{-2} + 2CH_2O \rightarrow H_2S + 2CO_2 + 2OH^-$$

H_2S is produced by the sulfate bacteria under anaerobic conditions (water-oil association). It is a component that is formed in the hypoxic environment of kerogen and sedimentary sulfur where gypsum and anhydride rocks exist in the geological section of the study area (Hussien and Gharbi, 2010b). During the process of hydrocarbon generation, the organic sulfur associated with kerogen and the primary sulfur associated with sediments can form H_2S and free organic sulfur compounds. The presence of anhydride is the key to the formation of H_2S through the thermal reduction process of sulfate (Ayangbenro et al., 2018; Ausma et al., 2017). Anhydrite sulfate reacts with hydrocarbons to form H_2S and carbon dioxide. Carbon dioxide is usually combined with calcium from anhydride to form calcite in rock pores, while excess carbon from hydrocarbons creates Pyro-bitumen (Walters et al., 2011). The (Orr, 1974) study showed that these reactions can occur in reduction conditions similar to the sulfur springs of the study area.

$$CaSO_4 + 2CH_2O \xrightarrow{Sulfate\ reducing\ bacteria} CaCO_3 + H_2S$$

where, $2CH_2O$ = organic matter.

Besides natural sources, sulfur can be originated from industrial operations such as combustion of fossil and biomass fuels. Also, the anthropogenic emissions of sulfur rised behind the natural emissions estimated at 70–100 Teragram per year (Ties and Luit, 2019). Majority of emmited sulfur, which is formed as SO_2, originates from industrial activities as the most polluting factor contributes to about total SO_2 emissions (Fioletov et al., 2016; Aguilar-Dodier et al., 2020). Whereas approximately 3 Teragram per year is emitted as form of H_2S (Long et al., 2016; Ties and Luit, 2019).

2. Methodology

The GPS was used to determine the coordinates of the observation

Table 1
H_2S gas at the monitoring site.

St. ID	Long Y-Easting	Lat. X-Northing	H_2S mg/L	Remarks
S1	297,303	3,724,264	6	Monitoring Test No.1 around Sayala
S2	297,305	3,724,262	10	Spring during October 25, 2018
S3	297,307	3,724,261	20	Air velocity
S4	297,312	3,724,262	24	= 17 km/h. NW
S5	297,314	3,724,265	26	4.72 m/s
S6	297,315	3,724,268	35	Pressure
S7	297,316	3,724,269	59	= 1.007 bar Air Temperature = 24 °C
S8	297,316	3,724,270	76	
S9	297,315	3,724,272	82	
S10	297,313	3,724,273	77	
S11	297,315	3,724,275	60	
S12	297,313	3,724,274	70	
S13	297,311	3,724,275	52	
S14	297,308	3,724,277	40	
S15	297,305	3,724,275	31	
S16	297,303	3,724,274	22	
S17	297,302	3,724,273	16	
S18	297,300	3,724,272	15	
S19	297,299	3,724,269	18	
S20	297,300	3,724,268	19	
S21	297,301	3,724,266	17	
S22	297,298	3,724,264	18	
S23	297,290	3,724,265	4	
S24	297,280	3,724,269	3	
S25	297,277	3,724,275	1	
S26	297,272	3,724,280	0	

St. ID	Long. Y-Easting	Lat. X-Northing	H_2S mg/L	Remarks
E1	298,924	3,722,357	1	Monitoring Test No.2 around Ilttayif
E2	298,922	3,722,359	6	Sp.
E3	298,916	3,722,362	5	Air velocity NW
E4	298,911	3,722,364	2	= 17 km/h.
E5	298,906	3,722,368	1	Pressure
E6	298,902	3,722,372	0	= 1.007 bar Air Temp.
E7	298,918	3,722,369	1	= 24 °C
E8	298,910	3,722,360	0	
E9	298,897	3,722,367	0	
E10	298,910	3,722,377	0	

St. ID	Long. Y-Easting	Lat. X-Northing	H_2S mg/L	Remarks
Sa1	297,300	3,724,280	14	Monitoring Test No.3 around Sayala
Sa2	297,304	3,724,277	20	Spring during November 22, 2018
Sa3	297,313	3,724,278	50	Air velocity
Sa4	297,321	3,724,279	1000	= 0.3 km/h.
Sa5	297,318	3,724,282	1000	0.08 m/s
Sa6	297,314	3,724,288	40	Pressure
Sa7	297,296	3,724,267	60	= 1.002 bar Air Temperature
Sa8	297,307	3,724,268	10	= 20 °C
Sa9	297,326	3,724,274	20	
Sa10	297,331	3,724,281	8	
Sa11	297,297	3,724,274	6	
Sa12	297,292	3,724,265	4	
Sa13	297,308	3,724,277	1	
Sa14	297,277	3,724,275	0	

Table 2
H_2S gas in the air around springs.

St. ID	Long. Y Easting	Lat. X Northing	H_2S Conc. (ppm)	St. ID	Long. Y-Easting	Lat. X-Northing	H_2S Conc. (ppm)
A1	296,668	3,725,063	7	S1	297,303	3,724,364	6
A2	296,984	3,725,426	0.0	S2	297,305	3,724,362	10
A3	296,888	3,725,708	0.0	S3	297,307	3,724,361	20
A4	297,378	3,725,305	0.0	S4	297,312	3,724,362	24
A5	298,051	3,724,998	0.0	S5	297,314	3,724,365	26
A6	297,225	3,724,350	0.0	S6	297,315	3,724,368	35
A7	297,889	3,724,570	0.0	S7	297,316	3,724,369	59
A8	298,395	3,724,079	0.0	S8	297,316	3,724,370	76
A9	298,028	3,724,073	0.0	S9	297,315	3,724,372	82
A10	298,066	3,723,643	0.0	S10	297,313	3,724,373	77
A11	299,532	3,723,256	0.0	S11	297,315	3,724,375	60
A12	299,777	3,722,885	1.0	S12	297,313	3,724,374	70
A13	300,209	3,722,655	0.0	S13	297,311	3,724,375	52
A14	300,451	3,723,164	1.0	S14	297,308	3,724,377	40
A15	301,001	3,723,502	0.0	S15	297,305	3,724,375	31
A16	300,017	3,723,915	0.0	S16	297,303	3,724,374	22
A17	299,478	3,724,187	0.0	S17	297,302	3,724,373	16
A18	298,884	3,723,311	0.0	S18	297,300	3,724,372	15
A19	299,113	3,722,620	0.0	S19	297,299	3,724,369	18
A20	298,800	3,724,006	0.0	S20	297,300	3,724,368	19
A21	297,540	3,723,811	0.0	S21	297,301	3,724,366	17
A22	296,372	3,725,244	0.0	S22	297,298	3,724,364	18
A23	297,266	3,724,800	0.0	S23	297,290	3,724,365	4
W1	297,319	3,724,280	100	S24	297,280	3,724,369	3
W2	296,926	3,724,199	7	S25	297,277	3,724,375	1
W3	296,911	3,724,150	6	S26	297,272	3,724,380	0
W4	297,102	3,724,273	5	E1	298,924	3,722,557	0
W5	296,917	3,724,081	4	E2	298,922	3,722,559	6
W6	296,874	3,724,068	4	E3	298,916	3,722,562	5
W7	296,605	3,724,634	0	E4	298,911	3,722,564	2
W8	296,772	3,724,975	0	E5	298,906	3,722,568	1
W9	296,878	3,725,143	0	E6	298,902	3,722,572	0
W10	296,857	3,725,356	0	E7	298,918	3,722,569	1
W11	297,046	3,725,553	0	E8	298,910	3,722,560	0
W12	296,777	3,725,755	0	E9	298,897	3,722,567	0

points of various field measurements. H_2S measurements of air were carried out using the Horiba APOA 360 E device after calibration prior to the measurements with an accuracy of 0.1 ppm within the monitoring network. The concentration of dissolved H_2S in spring water and wastewater was determined at 36 water samples after adding lead acetate to deposit it as lead sulfide for analyses.

The equipments that were used in the sampling were cleaned with deionized water. Water samples were collected using glass bottles that were carefully closed according to the procedure proposed by (USEPA, 2000). The direct measurement of discharge was calculated from water speed and cross-section area of the springs and wastewater canals according to the equation [Q (m^3/sec) = V (m/sec) *x* A (m^2)]. Based on the work procedure introduced by (Brikowski, 2011), a flow meter was used to determine the velocity of water in the canal. The concentration of H_2S was determined in the study area in 70 observation points (Table 1).

To assess H_2S emissions released from natural sources in the springs of sulfide water, and from the human activities related to wastewater. H_2S concentrations, in the study area, are recorded by three replicates per observation points selected as a suspected to contain effective H_2S emissions presence. In addition to a specific monitoring at 50 points (as shown in Table 2) distributed around the source of H_2S (S and E). Also, the direction and the speed of the wind has been taken into consideration (Horwell et al., 2005).

Depending on the pollutant dispersion hypothesis based on normal statistical distribution (Holmes and Morawska, 2006), using the principles of the Gaussian model, including dispersion coefficients (Pasquill, 1976; Gifford, 1976; Macdonald, 2003), the dispersion flux was determined by using the following formula (Ragazzi, 2017; EEA, 1998; Briggs and Haugen, 1975):

$C_{(x,y,z)} = [Q/U\ \pi\ \sigma_y\ \sigma_z]\ [\exp\{-(y^2/2\sigma_y^2)\}]\ [\exp\{-((z\text{-}H)^2/2\sigma_z^2)\}]$, where

C = steady-state concentration at a point (x, y, z), $\mu g/m^3$

Q = pollutant emission rate, μg/sec;

U = mean wind speed at release height; m/sec

σ_y, σ_z = standard deviation of lateral and vertical spread parameters, σy = Iy x; $\sigma_z = I_z x$; (m)

y = horizontal distance from plume centerline, m

x = downwind distance from plume source, m;

H = effective stack height (H = h + Δh) where h = physical stack height and Δh = plume rise;

z = vertical distance from ground level, m.

The results of the spatial analysis technique obtained from the Surfer11 program were used to explain air pollution phenomena of H_2S and to illustrate the behavior of H_2S concentration within its source area and the affected area. A model was developed between H_2S gas released into the atmosphere and dissolved H_2S in both springs and wastewater by determining the best correlation equation using the Curve Expert 1.4 software.

The Guidelines of Public Health (WHO, 2000), as well as the Ontario's Ambient Air Quality Criteria (OAAQC, 2012), have been adopted for the H_2S concentration limits and their physical symptoms. The lowest adverse impact of H_2S concentration is (0.01 mg/L or 0.007 mg/m^3) in which irritating odor complaints begin. Then concentration of 10–20 mg/L causes irritation of the eye. The concentration of 50–100 mg/L could be responsible for eye damage. The concentration of 150–250 mg/L cause olfactory loss. A concentration of 320–530 mg/L causes pulmonary edema with death risk. Finally, concentration of 530–1000 mg/L, which stimulates the central nervous system and stops breathing.

3. Results

3.1. Hydrogen Sulfide emissions

The H_2S measurements were carried out in the air and samples collected from both spring water and wastewater at the same time with 12 observation points by a total of 24 tests, including the flowing water of springs and it's mix with wastewater. The emission model was developed by applying the results of the measurements as shown in (Table 3). The correlation between the concentration of H_2S in air and its concentration in both spring water and wastewater (Fig. 2) was expressed in the formula of the exponential fit ($Y = a\ e^{bX}$), in which H_2S emission concentration can be predicted, where.

Y; H_2S concentration in Air (mg/1000 cc), X; H_2S concentration in water, a = 0.00015, b = 0.0107.

The concentration values of the emitted gas ranged from 0 to 7.75 mg/L (mg/1000 cm^3) compared to the concentration of dissolved gas in water ranging from 0 to 1000 mg/L.

The Emission Factor was calculated based on the concentration of the emitted gas (mg/L) per unit of discharge (l/sec). The H_2S emission factor from S and its mixed water with wastewater in Wadi Bassir was 0.0055 mg/L calculated at a discharge of 1 Liter/s, while the amount of the total emission rate of H_2S was reached 6.62 kg/year, calculated from the water discharge rate of 37.5 Liter/s (Table 3). This annual emission rate is much lower than that of geothermal power stations that reached hundreds of tons/year in Mexico (González-Acevedo and García-Zarate, 2018), 16,900 tons/year in Reykjavík-Iceland (Gunnarsson, 2013), and 494 tons/year in Sabalan-Iran (Hosseinzadeh, 2014).

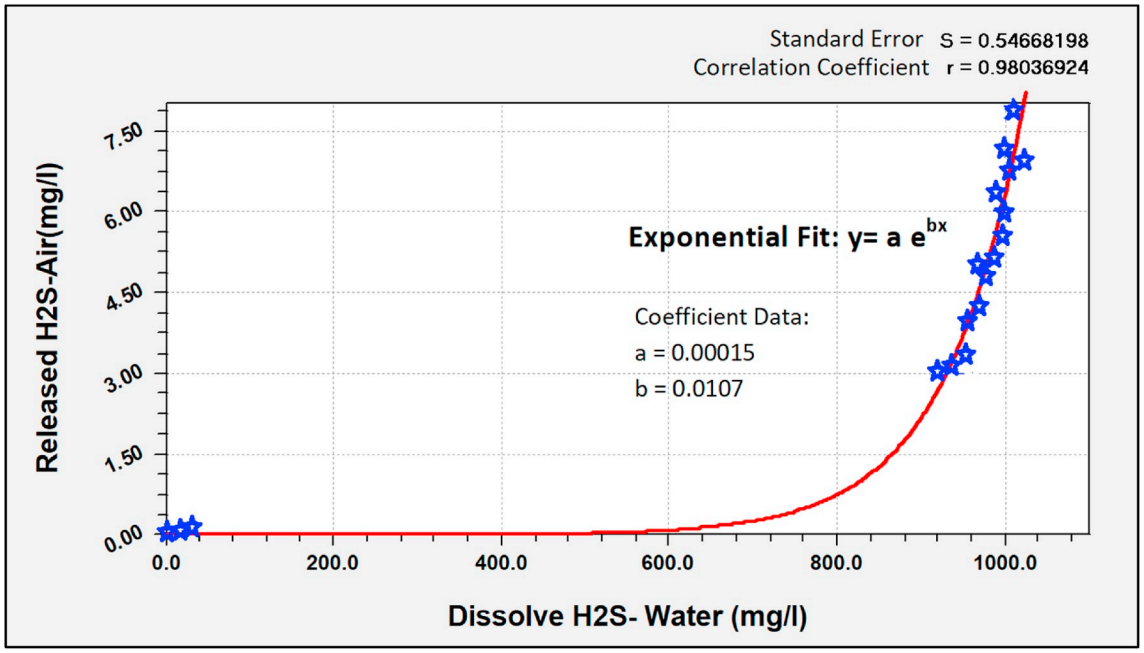

Fig. 2. Relation between dissolved H_2S in water and emitted H_2S gas to the atmosphere.

3.2. Characteristics and behavior of pollution plumes in unstable weather conditions

Air pollutants are dispersed depending on the speed and direction of the wind, as well as the coefficient and flux of dispersion based on the difference of concentration. Thus, the field measurements recoreded to study the behavior of pollution plumes, is performed concurrently around the sources of pollution (S and E) under same weather conditions, at a wind speed of 17 km/h towards NW, air temperature of 24 °C, and atmospheric pressure of 1.007 bars.

The distribution maps of the H_2S concentration (Figs. 3 and 4) derived from the field monitoring data at the springs sites during the unstable weather conditions (wind speed: 17 km/h) and confirmed the presence of H_2S gas emissions in the form of an oval plumes extended in the direction of the wind (NW) from the locations of H_2S plume spots.

A maximum gas concentration of 86 mg/L was recorded around S, which was classified on the basis of environmental impact, according to the proposals of WHO (2000) as H_2S pollution plume that exceeded the threshold of the unpleasant odor, eye irritation and within the limits of serious eye damage. While the maximum concentration of the gas plume around E was about 6 mg/L which was classified within the threshold of unpleasant odor and did not exceed the threshold of eye irritation.

The chemical gradient of H_2S concentration (mixing and dilution coefficient) was obtained from the spatial distribution map of gas emission within S region. Its values ranged between 0.14 mg/L per meter at the end of the plume and 18.41 mg/L per meter in the vicinity of the emission point. The concentration of gas has faded to zero at a distance of 40 m from the emission source in the western direction. While the amount of the chemical gradient of H_2S concentration within E region ranged from 0.1 mg/L/m to 6 mg/L/m. Also, the H_2S gas disappeared (zero concentration) within 20 m from the source of emission in the northwest direction.

The total natural mixing processes were studied under mechanical dispersion coefficient based on the mathematical relationship Dmx = α v (Berthouex and Brown, 2013), where, Dmx (m^2/sec): represents the mechanical dispersion coefficient, v (m/sec): average air speed and α: dynamic dispersivity (meter), represented by two types of vertical and

Table 3
H_2S gas concentration of the water and air in the same location.

St. ID	X Northing	Y Easting	Mean of the bi test H_2S (mg/l)		Remarks
			Water	Air	
W1	0297,319	3,724,280	1000	7.75	Spring Outflow(center)
W2	0296,926	3,724,199	1000	7	Spring Outflow (edges)
W3	0296,911	3,724,150	999	6	Spring Coarse
W4	0297,102	3,724,273	970	5	Spring Coarse
W5	0296,917	3,724,081	960	4	Spring Coarse
W6	0296,874	3,724,068	950	3	Spring Coarse
W7	0296,605	3,724,634	1	0	Spring Coarse
W8	0296,772	3,724,975	0	0	Spring Coarse
W9	0296,878	3,725,143	0	0	Mixed Springs water and Wastewater
W10	0296,857	3,725,356	0	0	Mixed Springs water and Wastewater
W11	0297,046	3,725,553	0	0	Mixed Springs water and Wastewater.
W12	0296,777	3,725,755	0	0	Wastewater
Mean	water flow line track	water flow line track	490	2.73	H_2S Emission Factor (mg/l) per water discharge (l/sec) = 2.73/490 = 0.0055 Rate of Emission = Spring water discharge x Emission Coef. = 37.5 Liter/s x 0.0055 mg/L = 0.21 mg/s = 6.62 kg/year

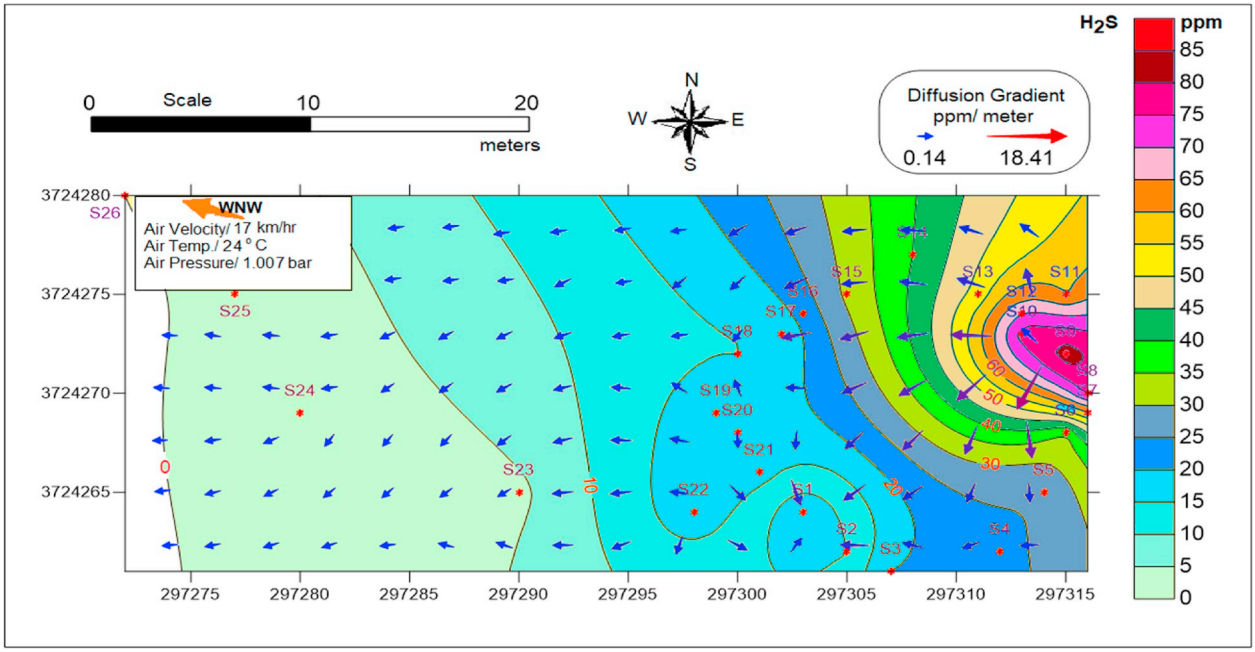

Fig. 3. Distribution map of the H_2S gas plume from S.

horizontal dynamic dispersivity based on so-called Gaussian model principles, which were determined from αz = Iz x, αy = Iy x, where x; represents the distance from the source (m), Iz; vertical pollution intensity, Iy; lateral pollution intensity.

Depending on average wind speed of 4.72 m/s (17 km/h) in the areas of H_2S release sources and compared with their corresponding values in Table 4, the vertical (Iz) and lateral pollution intensity (Iy) values were (0.065) and (0.165), respectively.

Accordingly, the values of the vertical dynamic dispersivity (αz) and the lateral dynamic dispersivity (αy) at the points that are far from the source by 25 m, reached 1.625 and 4.125 m, respectively. From the application of the above mentioned dynamic dispersivity values in equation (Dmx = α v), the vertical and lateral mechanical dispersion values reached about 7.67 and 19.47 m^2/s, respectively.

The dispersive flux of the H_2S gas from high to low concentration zone was calculated using Fick equation-1 [Fmx = -Dmx (∂c/∂x)], where Fmx; Dispersive flux, Dmx; mechanical dispersion coefficient, ∂c/∂x; Chemical gradient (change in concentration/distance).

The value of the H_2S chemical gradient (∂c/∂x) calculated from the spatial distribution map (Fig. 3) was 3.24 mg/L/m. Then, from the

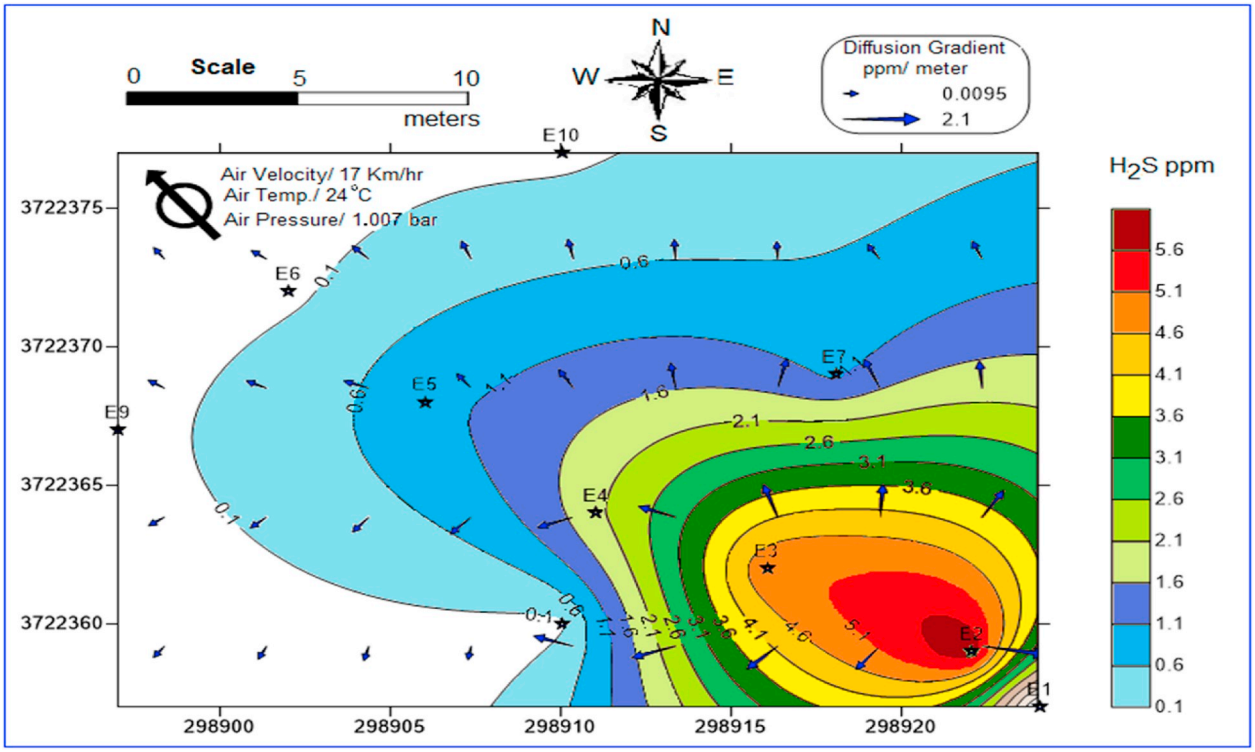

Fig. 4. Distribution of H_2S plume emission from E.

Table 4
Lateral and vertical turbulence intensities for different wind conditions (Berthouex and Brown, 2013).

Thermal Stratification	Lateral Intensity (Iy)	Average	Vertical Intensity (Iz)	Average	Air velocity m/sec
Extremely unstable	0.40–0.55	0.475	0.15–0.55	0.35	> 6
Moderately unstable	0.25–0.40	0.325	0.10–0.15	0.125	5–6
Near Stable/Unstable	0.10–0.25	0.165	0.05–0.08	0.065	3–5
Moderately stable	0.08–0.25	0.07	0.03–0.07	0.05	1–3
Extremely stable	0.03–0.25	0.04	≤0.03	0.02	< 1

Table 5
Mechanical Dispersion Coefficient and Dispersive flux of pollution plume.

Weather Condition	H_2S Plume	Intensity (I)		dynamic dispersivity (α) meter		Wind Velocity m/sec	Mechanical Dispersion D_{mx} = α v (m^2/sec)		Concentration Gradient ∂c/∂x (mg/l/m)or (g/m^3/m)	Dispersive flux F_{mx} = $-D_{mx}$ (∂c/∂x), (mg/cm^2 sec)	
		Lateral	Vertical	αy	αz		Lateral	Vertical		Lateral	Vertical
Unstable	S	0.165	0.065	4.125	1.625	4.72	19.47	7.67	3.24	63.08	24.85
	E								0.22	4.28	1.68
Extremely Stable	S	0.04	0.02	1	0.5	0.08	0.08	0.04	38	3.04	1.52

previous vertical and lateral mechanical dispersion values by using the first Fick equation, the values of the vertical and lateral dispersive flux within the plume pollution were 24.85 mg/cm^2 sec and 63.08 mg/cm^2 sec, respectively.

Also, from the spatial distribution map of H_2S around E (Fig. 4), the value of the H_2S gradient (∂c/∂x) was 0.22 mg/L/m, and from the application of Fick equation-1, the vertical and lateral dispersive flux values were 1.68 mg/cm^2 sec and 4.28 mg/cm^2 sec, (Table 5).

3.3. Characteristics and behavior of pollution plumes in extremely stable weather conditions

To identify the behavior of H_2S pollution plume during very stable weather conditions, the field measurements are carried out around the S region only since it has high H_2S emission (by 15 times higher than E region) which introduce the best explanation for H_2S plume behavior compared with E region.

The distribution map of H_2S concentration (Fig. 5) derived from the field monitoring data from S during extremely stable wind speed of 0.08 m/s, an air temperature of 20 °C and atmospheric pressure of 1.002 bars, confirmed that there is a plume of H_2S gas covering an area of 600 m^2 around emission site, with a minimum and maximum concentration values from 50 to 1000 mg/L.

The concentrations of plume pollution compared to the proposals of H_2S impact on health provided by the Health Organization (WHO, 2000; Chou, 2003), exceeded the threshold of eye irritation at the edges of the plume pollution and the dangerous impact on the eye within a radius of > 15 m from the center of the spring and causing loss of sense of smell and pulmonary embolism with the risk of death within a zone of radius between 10 and 15 m, and finally exceeded the threshold of stimulation of the central nervous system in the center of the flow and the area of diameter of 5 m.

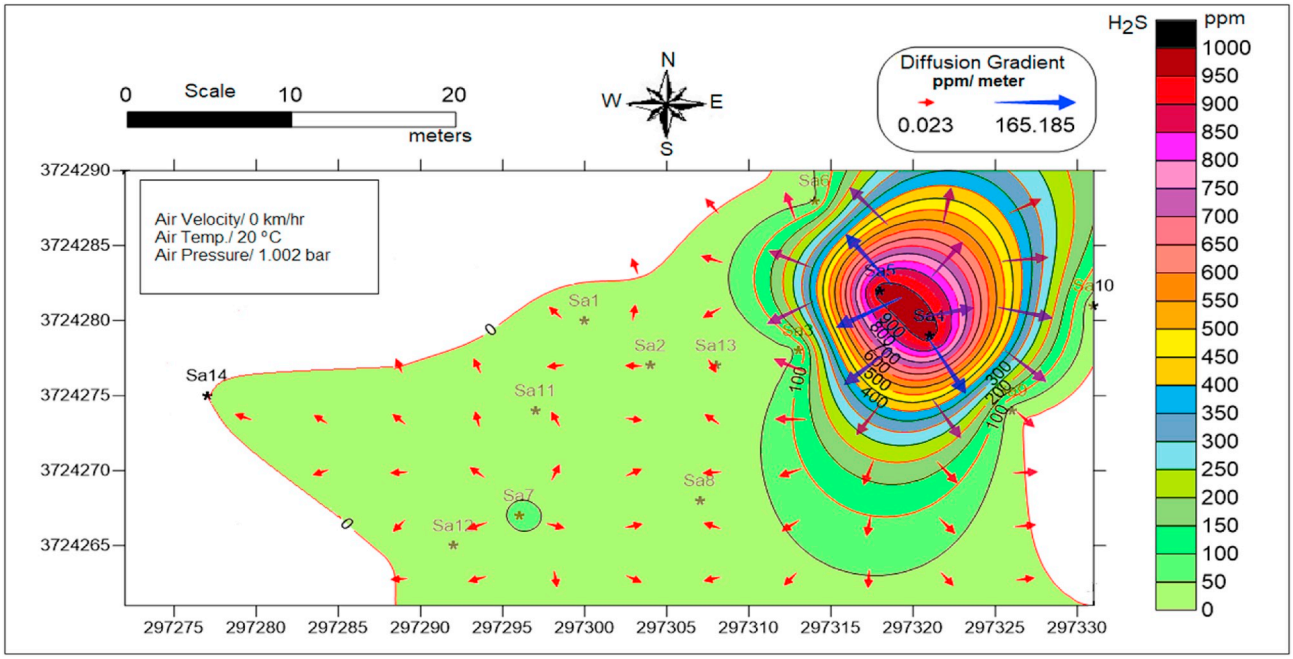

Fig. 5. Distribution map of the H_2S plume under extremely stable weather conditions.

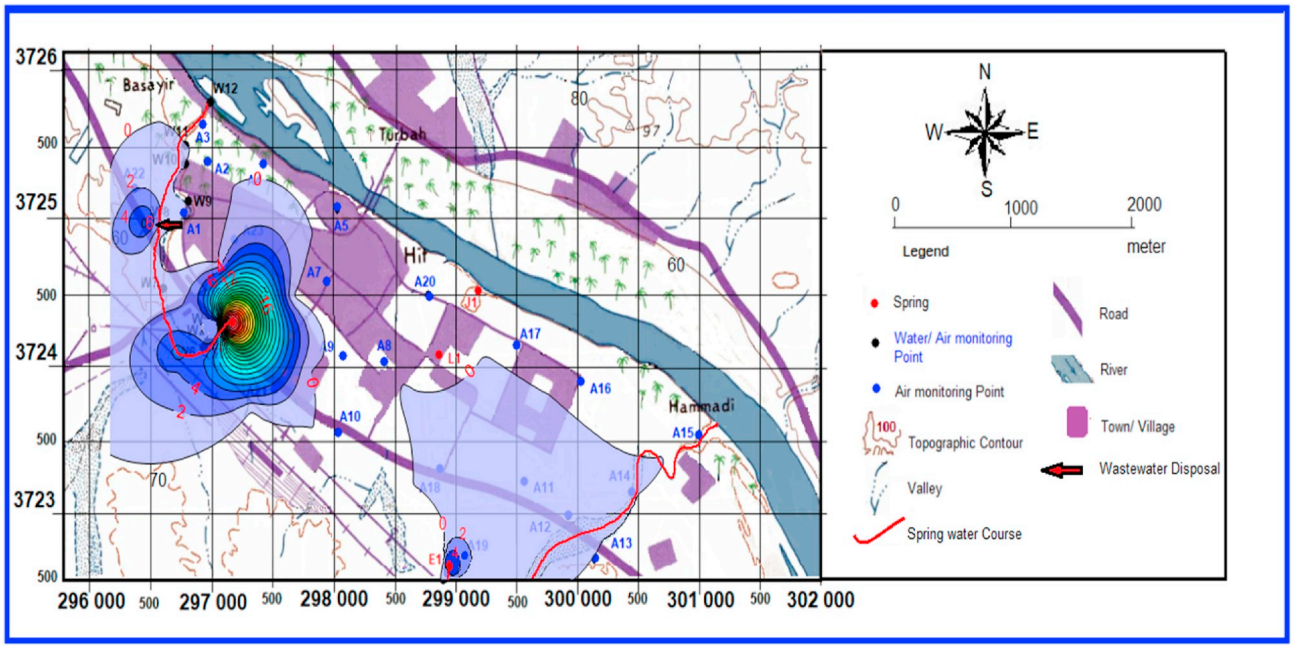

Fig. 6. Spatial distribution map of H_2S within Hit City.

The chemical gradient values of H_2S ranged from 0.023 mg/L/m at the end of the plume to 165.18 mg/L/m in the vicinity of the emission point, with an average value of 38 mg/L/m. The concentration of H_2S faded to zero far from the source of emission from a distance of 40 m in the western direction.

The value of the vertical pollution intensity (Iz) and the intensity of the lateral pollution (Iy) were (0.02) and (0.04) respectively, detected from the wind speed of 0.08 m/s, compared with their corresponding values in Table 4. The vertical dynamic dispersion values (αz = Iz x) and the lateral (αy = Iy x) at the observation points located 25 m from the source were about 0.5 and 1 m, respectively. Also, from the equation (Dmx = α v), the values of the vertical and lateral mechanical dispersion coefficient were about (0.04) and (0.08) m^2/sec, respectively. The dispersive flux within the pollution plume was about 1.52 and 3.04 mg/cm^2 sec for vertical and lateral pollution, respectively, calculated from the results of the H_2S gradient and the mechanical dispersion coefficients, using Fick equation-1, (Table 5, the field of extremely stable condition).

3.4. Features of Hydrogen Sulfide gas damage within Hit City

Field measurements of H_2S in both populated and the unpopulated areas of Hit City in conjunction with the field monitoring program are shown in the spatial distribution map (Fig. 6). Fig. 6 confirmed a close correlation between H_2S pollution plumes and the sources of gas release from SSp and their streams. Obviously shown that the H_2S concentration exceeded the proposed boundary of the disturbing odor around E. While its concentration exceeded Ontario's ambient air quality threshold of 0.01 mg/L/24 h (OAAQC, 2012) within the H_2S plume extended in the southeastern part of the study area.

H_2S concentrations around S exceeded the dangerous eye irritation threshold and the annoying odor threshold in a region extended with the H_2S plume, which corresponds to the spring water stream at a concentration of 5 mg/L to fade after 1 km of water flow. Also, The map revealed the presence of anomalous contamination within the threshold of unpleasant odor at the confluence point of municipal sewage with the spring water. The shape of the plume observed in the northwestern part of the city referred to a distribution pattern in which the concentration is reduced due to disperse until it reaches the threshold of the air quality limit over an area of 2.25 km^2.

The phenomenon of the damage and corrosion of the external parts of the cooling equipment (blackening of its heat exchangers) has been observed in the surrounding areas of H_2S release. The corrosion phenomenon varies depending on its location from the pollution plume because the concentration of H_2S exceeded the American Society Standard of 0.05 mg/L in humid environments (ISA, 1985). It should be noted that there is no uniform global standard for damage caused by H_2S concentration on air conditioners.

4. Conclusion

The results of this study indicate that the dispersion and behavior of pollution plume resulted from the continuous H_2S emissions from sulfuric spring and wastewater is 6.62 kg/year at an emission factor of 0.0055 (ppmgas/l/sec of water discharge). These results are compatible with the exponential fit model of atmospheric H_2S emissions. The spatial distribution maps of pollution plumes under unstable conditions indicated that the chemical gradient of H_2S emission in S region is 0.14 mg/L per meter and at the end of the plume is 18.41 mg/L per meter in the vicinity of the emission point. H_2S faded to zero at a distance of 40 m in the western direction. Whereas, the amount of the chemical gradient of H_2S at E region ranged from 0.1 mg/L/m to 6 mg/L/m then disappeared within 20 m in the northwest direction.

During the unstable conditions, the vertical (Iz) and lateral H_2S intensity (Iy) was (0.065) and (0.165), respectively. Also, the vertical dynamic dispersivity (αz) and the lateral dynamic dispersivity (αy) in the points that are far from the source by 25 m, are 1.625 and 4.125 m, with a vertical and lateral mechanical dispersion of about 7.67 and 19.47 m^2/s, respectively. Flux values of the vertical and lateral dispersive within the plume pollution during unstable conditions are 24.85 mg/cm^2 sec and 63.08 mg/cm^2 sec, respectively.

The region S is classified as a potential pollution point at the calm stable weather condition. However, Increased H_2S emissions rise due to the development of fractures caused by microseismic shocks. The increased concentration of H_2S exceeds the threshold of severe eye irritation around the source. The disturbing odor threshold occurs with the extension of a plume tongue that matched and faded with the effluent stream.

The distribution of the exposure area to H_2S is varied due to the impact of the wind speed where the H_2S plume recorded a high

concentration of maximum anomaly of 1000 mg/L during a very stable wind speed of 0.3 m/s. The maximum anomaly of H_2S decreased to 86 mg/L with an increase in wind speed of 7.24 m/s. That indicates the accumulation of H_2S concentration increased by 11.6 times when wind speed dropped by 15.7 times.

Data availability statement

All data generated or analyzed during this study are included in this published article.

Funding

This research received no grant from any funding agency.

Ethical approval

Not required.

References

Aguilar-Dodier, L.C., Castillo, J.E., Quintana, Penelope J.E., Montoya, Lupita D., Molina, Luisa T., Zavala, Miguel, Almanza-Veloz, V., Rodríguez-Ventura, J.G., 2020. Spatial and temporal evaluation of H2S, SO_2 and NH_3 concentrations near Cerro Prieto geothermal power plant in Mexico. Atmospheric Pollution Research 11 (1), 94–104. https://doi.org/10.1016/j.apr.2019.09.019.

Al Dulaymie, A., Hussien, B., Gharbi, M., Mukhlef, H., 2013. Balneological study based on hydrochemical aspects of the sulphate springs water (Hit - kubaiysa Region), Iraq. Arabian Journal of Geosciences 6 (3), 801–816. https://doi.org/10.1007/s12517-011-0385-5.

Ausma, T., Parmar, S., Hawkesford, M.J., De Kok, L.J., 2017. Impact of atmospheric H2S, salinity and anoxia on sulfur metabolism in Zea mays. In: De Kok, L.J., Hawkesford, M.J., Haneklaus, S.H., Schnug, E. (Eds.), Sulfur Metabolism in Higher Plants: Fundamental, Environmental and Agricultural Aspects. Springer, Dordrecht, pp. 93–101.

Austigard, A., Svendsen, K., Heldal, K., 2018. Hydrogen sulphide exposure in wastewater treatment. J. Occup. Med. Toxicol. 13, 10. https://doi.org/10.1186/s12995-018-0191-z.

Awadh, S., Abdul Al-Ghani, S., 2013. Assessment of sulfurous springs in the west of Iraq for balneotherapy, drinking, irrigation and aquaculture purposes. Environ. Geochem. Health. https://doi.org/10.1007/s10653-013-9555-6. ISSN 0269-4042.

Ayangbenro, Ayansina S., Olanrewaju, Oluwaseyi S., Babalola, Olubukola O., 2018. Sulfate-reducing bacteria as an effective tool for sustainable acid mine bioremediation. Front. Microbiol. 9. https://doi.org/10.3389/fmicb.2018.01986.

Bates, M.N., Crane, J., Balmes, J.R., Garrett, N., 2015. Investigation of hydrogen sulfide exposure and lung function, asthma and chronic obstructive pulmonary disease in a geothermal area of New Zealand. PloS One 10 (3), e0122062. https://doi.org/10.1371/journal.pone.0a122062.

Berthouex, P., Brown, L., 2013. Pollution Prevention and Control: Part I, Human Health and Environmental Quality, © 2013 Paul Mac Berthouex & Linfield C. Brown & bookboon.com ISBN 978-87-403-0526-5. 243pp.

Briggs, G., Haugen, D., 1975. Plume rise predictions. In: Haugen, D.A. (Ed.), Lectures on Air Pollution and Environmental Impact Analysis, American Meteorological Society. Amer. Meteor. Society, Boston 59 111.

Brikowski, T., 2011. Lab Notes, Hydrogeology Outdoor Laboratory. GEOS 4430 Geosci. Dep. Texas-Dallas, pp. 51p.

Chi, Qianru, Wang, Dongxu, Hu, Xueyuan, Li, Shiping, Li, Shu, 2019. Hydrogen sulfide gas exposure induces necroptosis and promotes inflammation through the MAPK/NF-κB pathway in broiler spleen. Article ID 8061823, 13 pages. https://doi.org/10.1155/2019/8061823.

Chou, C., 2003. Hydrogen Sulfide: Human Health aspects Concise International Chemical Assessment Document, vol. 53 World Health Organization, Geneva 2003.

Cornelius, G.F., Dagmar, R., Frank, B., Armin, Q., Jorg, F., 2001. Oxidation of reduced inorganic sulfur compounds by bacteria: emergence of a common mechanism? Appl. Environ. Microbiol. 67, 2873–2882. https://doi.org/10.1128/AEM.67.7.2873–2882.2001.

D'Alessandro, W., Aiuppa, A., Bellomo, S., Brusca, L., Calabrese, S., Kyriakopoulos, K., Liotta, M., Longo, M., 2012. Sulphur-gas concentrations in volcanic and geothermal areas in Italy and Greece: characterising potential human exposures and risks. J. Geochem. Explor. 131, 1–13. https://doi.org/10.1016/j.gexplo.2012.08.015.

EEA, 1998. Guidance Report on Preliminary Assessment under EC Air Quality Directives (Technical Report 11). European Environment Agency, pp. 67. 28.03.17. http://www.eea.europa.eu/publications/TEC11a.

Finnbjornsdottir, R.G., Carlsen, H.K., Thorsteinsson, T., Oudin, A., Lund, S.H., Gislason, Th, Rafnsson, V., 2016. Association between daily hydrogen sulfide exposure and incidence of emergency hospital visits: a population-based study. PloS One. https://doi.org/10.1371/journal.pone.0154946.

Fioletov, V.E., McLinden, C.A., Krotkov, N., Li, C., Joiner, J., Theys, N., et al., 2016. A global catalogue of large SO2 sources and emissions derived from the ozone monitoring system. Atmos. Chem. Phys. 16, 11497–11519. https://doi.org/10.5194/acp-16-11497-2016.

Gifford, F.A., 1976. Nucl. Saf. 17 (1), 68–86.

González-Acevedo, Z., García-Zarate, M., 2018. Geothermal Energy as an Alternative to Reduce Atmospheric Emissions and Provide Green Energy. https://doi.org/10.5772/intechopen.80759.

Gunnarsson, I., Reykjavík Energy, 2013. Geothermal gas emission from hellisheiði and nesjavellir power plants, Iceland. GRC Transactions 37, 2013.

Hamza, N.M., 1975. Regional Geological Mapping of AL-Tharthar-Hit-Qaser-AL-Khubaz Area. SOM. GDGMI, Baghdad, Unpublished Report (In Arabic).

Holmes, N.S., Morawska, L., 2006. A review of dispersion modeling and its application to the dispersion of particles: an overview of different dispersion models available. Atmos. Environ. 40–30, 5902–5928.

Horwell, C.J., Patterson, J.E., Gamble, J.A., Allen, A.G., 2005. Monitoring and mapping of hydrogen sulphide emissions across an active geothermal field: rotorua, New Zealand. J. Volcanol. Geoth. Res. 139, 259–269.

Hosseinzadeh, A., 2014. Air Quality Impact Assessment: H2S Dispersion Modeling for the Sabalan Geothermal Power Plant, NW-Iran, Orkustofnun, Grensasvegur 9, IS-108 Reykjavik. Iceland Report Number 15. United Nation University GTP. 24 P.

Hussien, B.M., 2010. Hydrogeological conditions within Al-anbar governorate. Journal of Anbar University for Pure Sciences 4 (3), 97–111 ISSN: 1991-8941.

Hussien, B., Gharbi, M., 2010a. Hydrogeologic condition within Abu-Jir Fault zone (Hit–Kubaiysa). Iraqi Journal of desert studies ISSN 2, 1994–7801 No. 2.

Hussien, B., Gharbi, M., 2010b. Hydro geochemical evaluation of the groundwater within Abu-Jir Fault zone. I.B.G.M, ISSN 1811-4539. SCGSM 6 No 1.

ISA, 1985. Environmental Conditions for Process Measurement and Control Systems: Airborne Contaminants. International Society for Automation, Research Triangle Park, North Carolina Standard ISA-71.04-1985. 12pp.

Jappinen, P., Vilkka, V., Marttila, O., Haahtela, T., 1990. Exposure to hydrogen sulphide and respiratory function. Br. J. Ind. Med. 47 (12), 824–828.

Kari, K Heldal, D Austigard, Åse, Svendsen, Kristin H., Einarsdottir, Elin, Lars Ole Goffeng, Liv Ingun Sikkeland, Karl-Christian Nordby, May 2019. Endotoxin and hydrogen sulphide exposure and effects on the airways among waste water workers in sewage treatment plants and sewer net system. Annals of Work Exposures and Health 63 (Issue 4), 437–447. https://doi.org/10.1093/annweh/wxz020.

Lantz, R.C., Orozco, J., Bogdanffy, M.S., 2003. Vinyl acetate decreases intracellular pH in rat nasal epithelial cell. Toxicol. Sci. 75, 423–431.

Legator, M.S., Singleton, C.R., Morris, D.L., Philips, D.L., 2001. Health effects from chronic low-level exposure to Hydrogen Sulfide. Arch. Environ. Health 56 (2), 123–131. https://doi.org/10.1080/00039890109604063.

Long, Yuyang, Yuan, Fang, Shen, Dongsheng, Feng, Huajun, Chen, Ting, 2016. Hydrogen sulfide (H2S) emission control by aerobic sulfate reduction in landfill. Sci. Rep. 6 (1). https://doi.org/10.1038/srep38103.

Macdonald, R., 2003. Theory and Objectives of Air Dispersion Modeling. University of Waterloo, Waterloo, pp. 27. www.engga.uwo.ca/people/esavory/MME474A_Part1.pdf.

Ontario's Ambient Air Quality Criteria (Oaaqc), 2012. Standards Development Branch. Ontario's Ministry of the Environment PIBS-6570e01. 15pp.

Orr, W.L., 1974. Changes in sulfur content and isotopic-ratios of sulfur during petroleum maturation—study of Big Horn basin Paleozoic oils. Bull. Am. Assoc. Petrol. Geol. 58 (11), 2295–2318.

Pasquill, F., 1976. Atmospheric dispersion parameters in Gaussian plume modeling, Part II. Possible Requirements for Change in the Turner Workbook Values. US Environmental Protection Agency, Research Triangle Park, NC EPA-600/4-76-030b.

Ragazzi, M., 2017. Air quality, monitoring, measuring, and modeling environmental hazards. Issued in Print and Electronic Formats. Apple Academic Press Inc. 9 Spinnaker Way Waretown, NJ 08758, Canada USA, pp. 266 978-1-77188-427-3 (hardcover).–ISBN 978-1-77188-428-0 (pdf).

Schneider, J.S., Tobe, E.H., Mozley Jr., P.D., Barniskis, L., Lidsky, T.I., 1998. Persistent cognitive and motor deficits following acute hydrogen Sulphide poisoning. Occup. Med. (Lond.) 48 (4), 255–260.

Selley, R.C., Sonnenberg, S.A., 2015. Elements of Petroleum Geology, third ed. .

Ties, A., Luit, J.D., 2019. Atmospheric H2S: impact on plant functioning. Front. Plant Sci. 10. https://doi.org/10.3389/fpls.2019.00743.

USEPA, 2000. National Water Quality Inventory: 2000 Report. EPA-841-R-02-001.

Walters, K.L., Beltran, R.E., Chae, D.H., Campbell, T.E., 2011. Displacement and disease: land, place and health among American Indians and Alaska natives. In: Burton, Linda M., Kemp, Susan P., Leung, Man Chui, Matthews, Stephen A., Takeuchi, David T. (Eds.), Communities, Neighborhood, and Health: Expanding the Boundaries of Place. Springer Science Business Media, LLC, Philadelphia, PA, pp. 163–199.

WHO, 2000. Air Quality Guidelines for Europe, second ed. World Health Organization Regional Publications, European Series Copenhagen.